Kinetics of formation and unimolecular decomposition of the FS(O 2)OOO radical

3 AUTHORS, INCLUDING:

Adela E. Croce
National University of La Plata
65 PUBLICATIONS **472** CITATIONS

SEE PROFILE

Carlos J. Cobos
National Scientific and Technical Research C...
126 PUBLICATIONS **3,054** CITATIONS

SEE PROFILE

Kinetics of formation and unimolecular decomposition of the FS(O$_2$)OOO radical

A.E. Croce, C.J. Cobos, E. Castellano *

Instituto de Investigaciones Fisicoquímicas Teóricas y Aplicadas (INIFTA), Departamento de Química, Facultad de Ciencias Exactas, Universidad Nacional de La Plata, Casilla de Correo 16, Sucursal 4, (1900) La Plata, Argentina

Abstract

The kinetics and mechanism of the 193 nm laser flash photolysis of FSO$_2$OF in the presence of O$_2$ and the bath gases N$_2$ and CF$_4$ were studied at 295 and 383 K. FSO$_3$ radicals and F atoms are formed in the primary photolytic process. Subsequently, the FO$_2$ radicals, produced by the combination of F with O$_2$, react with FSO$_3$ leading to the intermediate trioxide FS(O$_2$)OOOF. To explain the build-up of the room-temperature, time-resolved absorption signals observed at 450 nm, the formation of the novel FS(O$_2$)OOO radical, via F atom abstraction from the trioxide by FO$_2$, is proposed. FS(O$_2$)OOO then dissociates unimolecularly on a millisecond timescale into FSO$_3$ and O$_2$. This radical is not formed by recombination of FSO$_3$ with O$_2$. At 383 K, the faster thermal decomposition of FO$_2$ radicals precludes the formation of FS(O$_2$)OOO. © 1997 Elsevier Science S.A. All rights reserved.

1. Introduction

Fluorine fluorosulphate (FSO$_2$OF) exhibits hypofluorite properties and behaves as a powerful oxidizer. The thermal unimolecular decomposition of this compound leads to the formation of F atoms and fluorosulphate radicals (FSO$_3$) by breaking of the OF bond [1]. An identical primary process occurs in UV photolysis [2,3]. However, in this case, the FSO$_3$ radicals are initially formed in the B^{2}E electronic state, which is subsequently deactivated by collision to vibrationally excited levels of the electronic ground state and, finally, to thermalized radicals [4].

In the absence of F atom scavengers, the FSO$_2$OF photo-dissociation is followed by the recombination reaction

$$F + FSO_3 + M \rightarrow FSO_2OF + M \qquad (1)$$

which leads to its re-formation. The pressure (5–600 Torr of M $\equiv$ He, N$_2$, CF$_4$ and SF$_6$) and temperature (298–378 K) dependences of reaction (1) have recently been investigated [3]. The results have shown that this reaction is in the fall-off range between second- and third-order kinetics.

Several steady state studies carried out in our laboratory by Schumacher and coworkers [5–10] have demonstrated that, over the 263–523 K temperature range, the addition of

O$_2$ has no influence on reaction systems in which FSO$_3$ plays the central role. However, the FO$_2$ radical, which is produced mainly at lower temperatures by the termolecular reaction

$$F + O_2 + M \rightarrow FO_2 + M \qquad (2)$$

does not lead to a global kinetic effect under steady state conditions. Therefore the participation of this radical in these mechanisms should be elucidated. The kinetics of FO$_2$ reactions have recently been explored in direct experiments. These investigations have shown that FO$_2$ exhibits a varied reactivity with species such as CO, NO and NO$_2$ [11,12]. Therefore the reaction of the FO$_2$ radical with FSO$_3$ also appears to be of interest.

Continuing our time-resolved studies on the chemistry of the FSO$_3$ radical [3,4,13–20] [22], in the present work we have investigated the kinetics and mechanism of the photochemical decomposition of FSO$_2$OF at 193 nm in the presence of O$_2$. A mechanism which explains satisfactorily all the experimental observations is postulated. In this scheme, the intermediate species FS(O$_2$)OOOF and FS(O$_2$)OOO have been invoked for the first time.

2. Experimental technique

The excimer laser photolysis/absorption spectroscopy set-up has been described previously [3,4,13–22]. F atoms and

---

* Corresponding author.

FSO$_3$ radicals were generated with a quantum yield of essentially unity by the photodissociation of FSO$_2$OF with a pulsed ArF excimer laser (Lambda Physik EMG 101 MSC; emission at 193 nm) [3]. In the presence of sufficient O$_2$, the F atoms are quantitatively converted into FO$_2$ by reaction (2). As mentioned above, in O$_2$-free systems, reaction (1) is solely operative and, consequently, the temporal dependence of the FSO$_3$ absorbance monitored at 450 nm follows a strict second-order decay [3]. However, completely different absorption traces are found when O$_2$ is present, as shown in the following section. This indicates that FSO$_3$ is not the only transient species monitored under these conditions. The evolution of the intermediates was probed in real time by absorption spectroscopy using a 150 W Hanovia Xe arc lamp (901C-1) as light source. A crossed beam geometry between the photolytic and spectroscopic light beams was used in the present static experiments. After the reaction quartz cell (absorption path length, 2.4 cm), the analytical light was directed onto the entrance slit of a prism double monochromator (Zeiss MM12), equipped with a photomultiplier tube (RCA 1P28). Following amplification, the signals were monitored on a digital storage oscilloscope (Nicolet 2090). The determinations were made at spectral resolutions within the 3.0–4.0 nm wavelength range. Typically, five to ten laser shots were averaged to obtain signals with a signal-to-noise ratio suitable for quantitative kinetic analysis. The traces were subsequently transferred to a computer for storage and processing. A pyroelectric detector (Gentec ED-500) was employed to determine the laser pulse intensities incident on the reaction cell. The gases were handled in a conventional Pyrex vacuum system, and the pressures were measured with a calibrated pressure transducer (MKS Baratron, type 310CA) and with a quartz spiral gauge. Most of the experiments were conducted at an ambient temperature of 295 ± 2 K and a few at 383 ± 3 K.

FSO$_2$OF was synthesized by photolysis of a mixture of F$_2$ and SO$_3$ in a Pyrex reactor with a Hanau Q700 mercury arc lamp [23]. The reaction products, FSO$_2$OF and peroxydisulphuryl difluoride (F$_2$S$_2$O$_6$), were condensed at 195 K. The volatile fraction at 163 K resulting from the trap-to-trap distillations consisted of FSO$_2$OF. The purity of FSO$_2$OF was checked by IR spectrophotometry. The bath gases used have the following stated minimum purities: N$_2$ and O$_2$, 99.99% (La Oxígena); CF$_4$, 99.7% (Matheson). These gases were passed through a trap cooled at 153 K and stored in Pyrex flasks.

3. Results and discussion

To elucidate the reaction mechanism and to extract the kinetic data from the absorption signals, it is essential to know the nature of the species responsible for the absorption at 450 nm. FSO$_3$ shows a strong discrete band with an origin at 516 nm assigned to the C^{2}E ← X^{2}A$_2$ electronic transition [24]. This band is partially overlapped by a continuum which

decreases in intensity from approximately 470 to 340 nm [16,20,24]. However, FO$_2$ radicals formed by reaction (2) absorb weakly at the monitoring wavelength, the absorption cross-sections for the FSO$_3$ and FO$_2$ radicals being σ(FSO$_3$) = 3.64 × 10^{-18} cm^2 molecule^{-1} [13] and σ(FO$_2$) ≈ 1.4 × 10^{-19} cm^2 molecule^{-1} [25]. However, the kinetic evidence presented here indicates that another transient species is mainly responsible for the signals detected in the 193 nm laser flash photolysis of FSO$_2$OF–O$_2$–N$_2$ or CF$_4$ mixtures. Fig. 1 shows the time dependence of the absorbance monitored at 450 nm. The marked decay is ascribed to both the collisional removal of the generated vibrationally excited FSO$_3$ radicals [4] and to reaction (1) [3]. As the F atoms are quantitatively converted into FO$_2$ via reaction (2) within less than 25 μs, the concentration of FSO$_3$ radicals at the minimum absorption in Fig. 1 is higher than that observed in the absence of O$_2$. Furthermore, FSO$_3$ radicals are not substantially removed by the self-reaction

$$FSO_3 + FSO_3 \rightarrow F_2S_2O_6 \tag{3}$$

on this timescale [13,15]. A slight increase in the absorbance is observed in Fig. 1 towards longer times. Indeed, as shown in Fig. 2(b), the signal recorded on a millisecond timescale behaves quite differently with a pronounced build-up followed by a decay. If this rise is attributed to FSO$_3$, the concentration of these radicals should increase with respect to the initial value by a factor of greater than two (as calculated from the ratio of the absorbances at about 1.8 ms and 40 μs). However, the FSO$_3$ concentration at the absorbance maximum of Fig. 2(b) is reduced by a factor of close to two by reaction (3) [13]. In addition, no plausible secondary reaction could lead to an increase in FSO$_3$ concentration in the present experimental conditions. It should be noted that reaction FO$_2$ + FSO$_2$OF → F$_2$O$_2$ + FSO$_3$ is endothermic by about 55 kJ mol^{-1} [3,26] and consequently can be ruled out. Therefore FO$_2$ and thermalized FSO$_3$ radicals are essentially the initial reactants of the system over 50 μs, and the observed absorption rise must correspond to the formation and removal of an intermediate species different from FO$_2$ or FSO$_3$. This
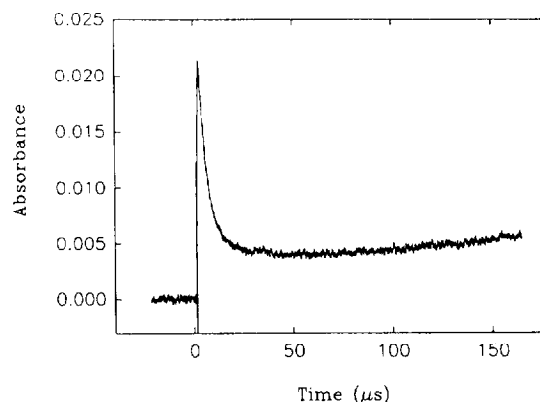

Fig. 1. Time-resolved absorbance monitored at 450 nm resulting from the 193 nm photolysis of 14.4 Torr of FSO$_2$OF in the presence of 50.4 Torr of O$_2$ and 48.5 Torr of N$_2$ at 295 K.
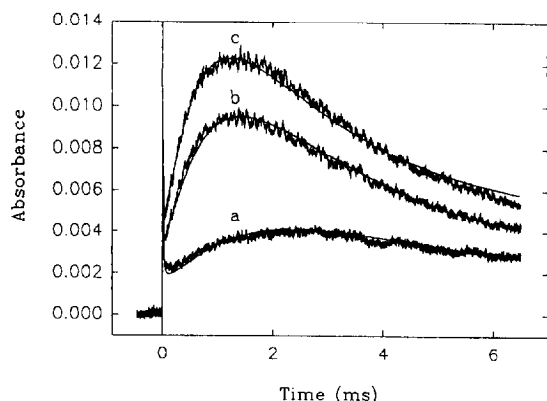
Fig. 2. Time-resolved absorbance monitored at 450 nm resulting from the 193 nm photolysis of FSO_2OF in the presence of O_2 and N_2 at 295 K: (a) $FSO_2OF = 14.6$ Torr, $O_2 = 11.4$ Torr, $N_2 = 90.6$ Torr; (b) $FSO_2OF = 14.4$ Torr, $O_2 = 50.4$ Torr, $N_2 = 48.5$ Torr; (c) $FSO_2OF = 13.7$ Torr, $O_2 = 100.7$ Torr, $N_2 = 0$ Torr. The full lines are the results of the modelling described in the text.
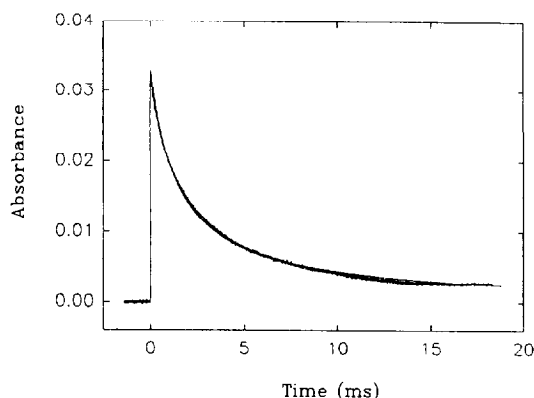

Fig. 3. Time-resolved absorbance monitored at 450 nm resulting from the 193 nm photolysis of 4.8 Torr of $F_2S_2O_6$ in the presence of 707.1 Torr of O_2 at 295 K. The full line is the result of the second-order decay fitting described in the text.

species could be formed through the reaction of FSO_3 with either O_2 or FO_2.

Firstly, indirect experiments indicate that FSO_3 does not react with O_2 [5–10]. The photolysis of $F_2S_2O_6$ at 193 nm (FSO_3 quantum yield close to 2 molecules quantum $^{-1}$ [13]) in the presence of O_2 allows for a direct verification of the indirect studies. Fig. 3 shows an absorbance trace obtained at 450 nm after the photodissociation of 4.8 Torr of $F_2S_2O_6$ diluted in 707.1 Torr of O_2. In contrast with the pseudo-first-order decay of the FSO_3 absorbance, expected for a reaction between FSO_3 and O_2, a strict second-order kinetic behaviour is observed over the whole timescale. The full line was calculated using a rate coefficient of 4.1×10^{-14} cm^3 molecule^{-1} s^{-1}. This value is in very good agreement with the limiting high pressure rate coefficient $k_{rec,\infty} = (4.5 \pm 0.2) \times 10^{-14}$ cm^3 molecule^{-1} s^{-1} determined for the recombination reaction (3) [13,15]. This finding clearly demonstrates that FSO_3 does not react with O_2 and, consequently, O_2 merely behaves as a third body in this experiment. In order to interpret this behaviour, the standard enthalpy change (ΔH°) for the reaction $FSO_3 + O_2 \rightarrow FS(O_2)OOO$

was estimated. According to the group additivity rules of Benson [27], the standard enthalpy of formation for the $FS(O)_2OOO$ radical is given by $\Delta H_f^\circ(FS(O)_2OOO) \approx \Delta H_f^\circ(FSO_3) + \Delta H_f^\circ[O-(O)_2] + \Delta H_f^\circ[O-(O)(S)]$. After simplifications and using the group contribution values $\Delta H_f^\circ[O-(O)_2] = 80$ kJ mol^{-1} [27,28] and $\Delta H_f^\circ[O-(O)(S)] \approx \Delta H_f^\circ[O-(O)(SO_2)] = 13$ kJ mol^{-1} [29], the value $\Delta H^\circ \approx 93$ kJ mol^{-1} is derived. $\Delta H^\circ \approx 68$ kJ mol^{-1} is obtained if the value $\Delta H_f^\circ[O-(O)_2] = 55$ kJ mol^{-1} [30] is employed. Therefore this endothermicity for the addition of O_2 to FSO_3 explains the observed absence of reactivity. Some other similar cases have been reported. Indeed, quantum chemical calculations predict standard enthalpy changes of 28.6, 49.3 and 35.3 kJ mol^{-1} [30] and 54.4 kJ mol^{-1} [31] for the reactions $RO + O_2 \rightarrow ROOO$ where $R \equiv H$, CH_3, CF_3 and Cl respectively.

Secondly, the dependence of the absorbance rise on the O_2 pressure at a constant total pressure, observed in the present experiments as shown in Fig. 2, indicates that the monitored transient species is related to the FO_2 formed in reaction (2). This is supported by the fact that the signals detected at a constant O_2 pressure depend on CF_4 pressure as presented in Fig. 4. Therefore both sets of experiments demonstrate that the observed intermediate is proportional to the FO_2 concentration. However, the intermediate decay is independent of O_2 and the total pressure (see below). In this way, the formation of the $FS(O_2)OOOF$ trioxide via the association reaction

$$FSO_3 + FO_2 + M \rightarrow FS(O_2)OOOF + M \qquad (4)$$

is proposed. To our knowledge, $FS(O_2)OOOF$ has not been reported previously. However, stable trioxide compounds, such as CF_3OOOCF_3 [32,33] and SF_5OOOSF_5 [34–36], have been synthesized. Evidence suggests that other trioxides would have stable minimum energy structures. Indeed, ther-
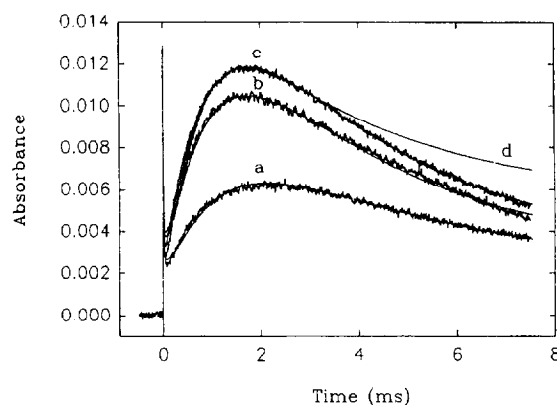

Fig. 4. Time-resolved absorbance monitored at 450 nm resulting from the 193 nm photolysis of FSO_2OF in the presence of O_2 and CF_4 at 295 K: (a) $FSO_2OF = 15.0$ Torr, $O_2 = 50.9$ Torr, $CF_4 = 0$ Torr; (b) $FSO_2OF = 15.2$ Torr, $O_2 = 50.1$ Torr, $CF_4 = 49.6$ Torr; (c) $FSO_2OF = 14.9$ Torr, $O_2 = 50.1$ Torr, $CF_4 = 96.7$ Torr. The full lines which fit the signals are the results of the modelling described in the text. Full line d was calculated by replacing reaction (6) with reaction (13) in the mechanism.

mochemical calculations indicate that some alkyl trioxides have sufficient stability to be isolable below room temperature [37], and ab initio calculations predict stable configurations for simpler compounds, such as the isomers ClOOO [31], HOOOCl [38,39] and even HOOOOCl [40]. Moreover, the enthalpy of formation and optimized geometry of the related compound $FS(O_2)OS(O)F$ have recently been estimated by PM3 calculations [41]. It is well known that the fluorosulphuryl fluoroperoxide $FS(O_2)OOF$, formed by recombination of FSO_3 and OF radicals, is thermally stable at temperatures below 323 K [42,43]. ^{17}O NMR measurements indicate that this compound is formed in the reaction between dioxygen difluoride F_2O_2 and SO_2 at 113 K (sulphuryl fluoride F_2SO_2 is the main reaction product) through a reaction similar to Eq. (4), namely $FSO_2 + FO_2 + M \rightarrow FS(O_2)OOF + M$ [44]. Hence the stabilization of $FS(O_2)OOOF$, due to the electron-withdrawing effect of the electronegative $FS(O_2)O-$ group, at least during the millisecond timescale of the present experiments, appears to be reasonable.

The absorption spectra of $F_2S_2O_6$ and FSO_3 are not superimposed. As mentioned above, the FSO_3 spectrum exhibits diffuse bands above 340 nm, while the dimer presents a continuous absorption below 270 nm [7,24]. On the basis of this evidence, it seems unlikely that the closed-shell compound $FS(O_2)OOOF$ presents such a strong absorption as shown by the experiments at 450 nm. Therefore the open-shell species $FS(O_2)OOO$, formed in the abstraction process

$$FS(O_2)OOOF + FO_2 \rightarrow FS(O_2)OOO + F_2O_2 \qquad (5)$$
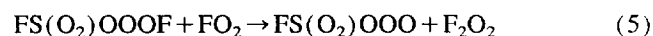
is proposed to interpret the time-resolved absorbances of Figs. 2 and 4. Due to the likeness of $FS(O_2)OOO$ and FSO_3, similar absorption spectra for these radicals could be expected. CNDO calculations suggest that the observed absorption system of FSO_3 involves essentially the promotion of an electron from the lone-pair molecular orbitals of e symmetry (centred mainly on the oxygen atoms) to the a_2 orbital [45]. Furthermore, the present experimental evidence (see below) indicates that the presence of the $-OO$ group in $FS(O_2)OOO$ leads to an enhancement of the absorption cross-section with respect to that of the FSO_3 radical. The $FS(O_2)OOO$ radical has not been reported previously. However, the formation of CF_3OOO radicals has been detected by electron spin resonance (ESR) during the photolysis of CF_3OOCF_3 in the presence of a small amount of O_2 enriched in ^{17}O at 77 K [46]. A decrease in the lifetime of this radical from about 15 min to 3 s was observed when the temperature was raised from 77 to 93 K. The thermochemistry of this and other polyoxy radicals has been investigated theoretically in Ref. [30].

After formation, we assume that $FS(O_2)OOO$ decomposes unimolecularly

$$FS(O_2)OOO + M \rightarrow FSO_3 + O_2 + M \qquad (6)$$
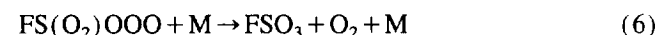
regenerating FSO_3 which, a posteriori, leads to the formation, via reaction (3), of the reaction product $F_2S_2O_6$. The possi-

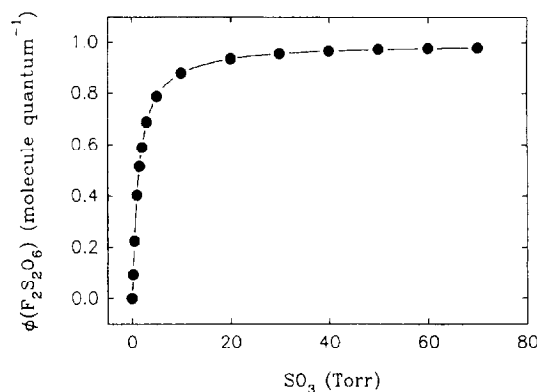Fig. 5. Calculated quantum yield of formation of $F_2S_2O_6$ during the photolysis of F_2 in the presence of SO_3 and N_2 at 298 K ($F_2 = 100$ Torr, $SO_3 + N_2 = 70$ Torr): ●, simulations with reactions (1), (3), (7) and (8).

bility of the consumption of $FS(O_2)OOO$ by self-reaction will be discussed later.

Although $FS(O_2)OOO$ could also be formed by F atom abstraction from $FS(O_2)OOOF$ by FSO_3, experimental evidence [2,5], which will be discussed later, allows this reaction to be discarded. Indeed, during the photochemical decomposition of F_2 at 365 nm in the presence of sufficiently high SO_3 pressures, the F atoms generated

$$F_2 + h\nu \rightarrow 2F \qquad (7)$$

recombine very rapidly to form FSO_3 [5]

$$F + SO_3 + M \rightarrow FSO_3 + M \qquad (8)$$

Finally, the FSO_3 radicals dimerize according to reaction (3) to form $F_2S_2O_6$ with a quantum yield $\phi(F_2S_2O_6)$ close to unity. As the SO_3 concentration diminishes, reactions (1) and (8) compete for the F atoms and, consequently, $\phi(F_2S_2O_6)$ decreases. Fig. 5 shows the results of a steady state modelling simulation which reproduces the experimental observations of Ref. [5] at SO_3 pressures higher than 20 Torr. In this calculation, reactions (1), (3), (7) and (8) [9] have been employed. The rate equations resulting from this mechanism were numerically integrated using a fourth-order Runge–Kutta algorithm. The values $k_1 = 5.1 \times 10^{-11}$ cm^3 molecule^{-1} s^{-1} [3] and $k_3 = 4.5 \times 10^{-14}$ cm^3 molecule^{-1} s^{-1} [13,15] have been employed for reactions (1) and (3) respectively. For reaction (8), a value $k_8 = 1.5 \times 10^{-12}$ cm^3 molecule^{-1} s^{-1} was obtained from the ratio $k_8 / k_1 = 3.0 \times 10^{-2}$ [2] and the above k_1 value. Similar conclusions may be extracted from the study of the photolysis of FSO_2OF at 254 nm in the presence of SO_3 [2]. In both studies, the addition of O_2 and inert gases has no influence on $\phi(F_2S_2O_6)$. At sufficiently high O_2 pressures, reactions (2) and (8) compete for the F atoms. However, under the minute timescale of the experiments of Refs. [2] and [5], the formation and decomposition of $FS(O_2)OOOF$ and $FS(O_2)OOO$, of course, do not play any role. Thus, using reactions (1)–(3) and (7)–(11), $\phi(F_2S_2O_6)$ as a function of O_2 pressure was calculated.

Table 1
Reaction mechanism and rate coefficients

Reaction	Rate coefficient[a]	Reference
$F + FSO_3 + M \rightarrow FSO_2OF + M$[b]	$k_0 = 5.2 \times 10^{-28}(T/300)^{-3.1}[N_2]$	[3]
	$k_0 = 1.1 \times 10^{-27}(T/300)^{-3.1}[CF_4]$	[3]
	$k_\infty = 7.2 \times 10^{-11}(T/300)^{0.23}$	[3]
$F + O_2 + M \rightarrow FO_2 + M$[c]	$k_0 = 5.8 \times 10^{-33}(T/300)^{-1.7}[N_2] \text{ s}^{-1}$	[48]
$FSO_3 + FO_2 + M \rightarrow FS(O_2)OOOF$	$(3.9 \pm 0.5) \times 10^{-13}$	This work
$FS(O_2)OOOF + FO_2 \rightarrow FS(O_2)OOO + F_2O_2$	$(6.4 \pm 0.7) \times 10^{-12}$	This work
$FS(O_2)OOO + M \rightarrow FSO_3 + O_2 + M$	$(6.0 \pm 1.5) \times 10^2 \text{ s}^{-1}$	This work
	$10^{13} \exp[-(7045 \pm 100)/T] \text{ s}^{-1}$	This work
$FSO_3 + FSO_3 \rightarrow F_2S_2O_6$	$k_\infty = 4.5 \times 10^{-14}(T/300)^{1.0}$	[13,15]
$FO_2 + M \rightarrow F + O_2 + M$[c]	$1.03 \times 10^{-5}T^{-1.25} \exp(-5990/T)[N_2] \text{ s}^{-1}$	[48]
$FO_2 + FO_2 + M \rightarrow F_2 + 2O_2 + M$[d]	$2.4 \times 10^{-33}[M]$	[50]
$F_2O_2 + O_2 \rightarrow 2FO_2$	$8.4 \times 10^{-8} \exp(-6520/T)$	[51]

[a]Units of cm^3 molecule^{-1} s^{-1} unless otherwise indicated. Rate coefficients are at 295 K unless an explicit temperature dependence is indicated.
[b]The rate coefficients employed in the simulation were obtained with the reduced fall-off expression of Ref. [3] and the indicated k_0 and k_∞ values. Rate coefficients equal to those for $M \equiv N_2$ and CF_4 were assumed for $M \equiv O_2$ and FSO_2OF respectively.
[c]Rate coefficients for $M \equiv O_2$ are assumed to be identical to those of $M \equiv N_2$. For $M \equiv FSO_2OF$ and CF_4, rate coefficients 2.4-fold higher than the corresponding values for $M \equiv N_2$ were employed [3].
[d]Expression employed for $M \equiv O_2$ and N_2. For $M \equiv FSO_2OF$ and CF_4, the rate coefficients were increased by a factor of 2.4 [3].
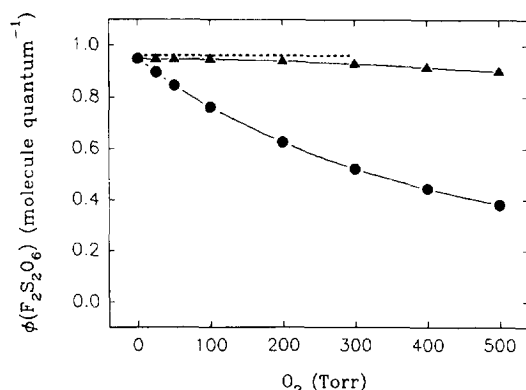

Fig. 6. Calculated quantum yield of formation of $F_2S_2O_6$ during the photolysis of F_2 in the presence of SO_3, O_2 and N_2 at 298 K ($F_2 = 100$ Torr, $SO_3 = 25$ Torr, $O_2 + N_2 = 500$ Torr): – – –, experimental results from Ref. [5]; ▲, simulations with reactions (1)–(6) and (7)–(11); ●, simulations with reactions (1)–(4), (6) and (7)–(12).
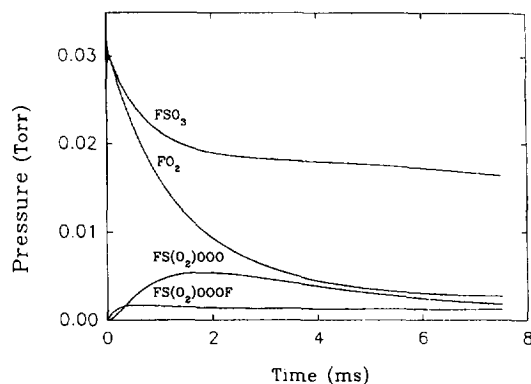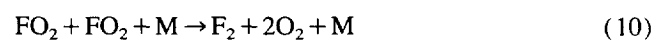

Fig. 7. Calculated pressures of FO_2, FSO_3, $FS(O_2)OOO$ and $FS(O_2)OOOF$ as a function of time for the experiment of Fig. 4(c).

$$FO_2 + M \rightarrow F + O_2 + M \qquad (9)$$

$$FO_2 + FO_2 + M \rightarrow F_2 + 2O_2 + M \qquad (10)$$

$$F_2O_2 + O_2 \rightarrow 2FO_2 \qquad (11)$$

Other fluorine oxide reactions, such as the reactions of F atoms with FO_2 [47,48] or F_2O_2 [47], or the thermal dissociation of F_2O_2 [49], are negligibly slow under our experimental conditions. The employed rate coefficients are given in Table 1 and the results are depicted in Fig. 6. In agreement with the experimental quantum efficiency for $F_2S_2O_6$ formation of 0.97 molecule quantum^{-1} (within 5%) between 3 and 300 Torr of O_2 from Ref. [5], a $\phi(F_2S_2O_6)$ value decreasing slightly from 0.95 to 0.90 molecule quantum^{-1} when the O_2 pressure was changed from 0 to 500 Torr is calculated.

As mentioned above, in addition to reaction (5), the $FS(O_2)OOO$ radical can also be generated through reaction (12)

$$FS(O_2)OOOF + FSO_3 \rightarrow FS(O_2)OOO + FSO_2OF \qquad (12)$$
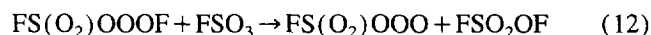
The present laser flash photolysis experiments do not allow us to choose between reactions (5) and (12). However, it is observed that, in reaction (12), one FSO_3 radical is consumed to form FSO_2OF, which is not appreciably photolysed at 365 nm [16]. As a consequence, $\phi(F_2S_2O_6)$ should decrease at large O_2 pressures. The calculations presented in Fig. 6 show a pronounced decrease in $\phi(F_2S_2O_6)$ with O_2 pressure and therefore, according to the results of Schumacher and coworkers [2,5], the occurrence of reaction (12) can be discarded.

It is convenient at this stage to describe the results of the numerical simulation of the reaction mechanism made up of reactions (1)–(6) and (9)–(11). The time-resolved absorbances shown in Figs. 2 and 4, and others not presented here, are well reproduced by employing the rate coefficients given in Table 1. In order to illustrate the temporal evolution of the central species of the system, typical dependences for the pressures of FO_2, FSO_3, $FS(O_2)OOO$ and $FS(O_2)OOOF$ on time are illustrated in Fig. 7. The best values for the rate

coefficients k_4, k_5 and k_6 were obtained from a non-linear least-squares fit of the simulated $FS(O_2)OOO$ formation and decay curves to the experimental profiles. We found that k_4 and k_6 are, under the present conditions, independent of the total pressure, and therefore are probably very close to their respective high pressure limits. The k_4 value is similar to the upper limit reported for the reaction $FC(O)O + FO_2 \rightarrow$ products of 2×10^{-13} cm^3 molecule^{-1} s^{-1} [52]. Furthermore, as expected, k_4 is smaller than the rate coefficient for the $FSO_3 + OF \rightarrow FS(O_2)OOF$ recombination reaction estimated as $\geq 50k_3 = 2.3 \times 10^{-12}$ cm^3 molecule^{-1} s^{-1} [13,15,42]. Statistical adiabatic channel model [53,54] calculations performed for this reaction lead to $k_{rec,\infty} = 3.5 \times 10^{-12}$ cm^3 molecule^{-1} s^{-1}, which is only 20% higher than the rate coefficient evaluated from the analysis of the fall-off curve at an N_2 pressure of 150 Torr [55]. The lack of molecular information on the trioxide molecules involved in reaction (4) precludes a similar theoretical study. However, because of the major complexity of these molecular species, a smaller pressure dependence could, in principle, be expected for reaction (4). These facts support the independence of reaction (4) of the total pressure which results from the present study.

In the absence of further information, pressure effects similar to those for the reaction between FSO_3 and OF can be expected for the dissociation of $FS(O_2)OOO$ into FSO_3 and O_2 through reaction (6). The fall-off estimated in the preceding paragraph for the $FSO_3 + OF$ recombination is comparable with the estimated uncertainty in k_6 given in Table 1.

As mentioned above and shown in Fig. 1, the marked increase in the absorbance attributed to the $FS(O_2)OOO$ radical is located at the time at which the FSO_3 concentration decreases due to the recombination reaction (3). This indicates that the $FS(O_2)OOO$ radical exhibits an absorption cross-section much greater than that of the FSO_3 radical. As a result of all the experiments analysed, the value $\sigma(FS(O_2)OOO) = (4.4 \pm 0.3) \times 10^{-17}$ cm^2 molecule^{-1} is obtained at 450 nm.

In Fig. 4, the results of a numerical simulation, carried out by employing the self-reaction

$$FS(O_2)OOO + FS(O_2)OOO \rightarrow 2FSO_3 + 2O_2 \qquad (13)$$
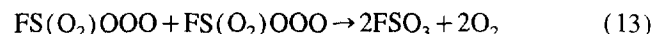
in the reaction scheme instead of reaction (6), are presented. Using the rate coefficients of Table 1 and a value of $k_{13} = 1.5 \times 10^{-12}$ cm^3 molecule^{-1} s^{-1}, only a limited portion of the upper part of the signal may be reproduced. It is observed that, at times longer than about 3.5 ms, the calculated absorbances largely overestimate the experimental. Therefore the most probable fate of $FS(O_2)OOO$ is thermal decomposition according to reaction (6). The exothermicity of reaction (6) supports the presence of an activation barrier to deoxygenation. Thus, assuming that the reaction proceeds through a tight transition state located at the maximum of the barrier and with a typical pre-exponential factor of 10^{13} s^{-1} [56], an activation energy of $E_{a,6} = 58.6 \pm 0.8$ kJ mol^{-1} is

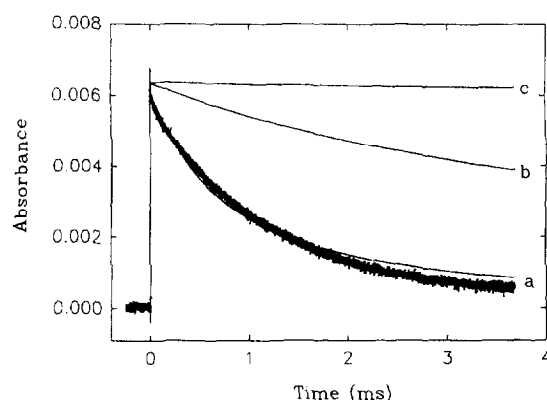Fig. 8. Time-resolved absorbance monitored at 450 nm resulting from the 193 nm photolysis of FSO_2OF in the presence of O_2 at 383 K ($FSO_2OF = 2.5$ Torr, $O_2 = 755.1$ Torr): (a) modelling with reactions (1)–(6) and (9)–(11); (b) modelling with reactions (2)–(6) and (9)–(11); (c) modelling with reactions (2), (4)–(6) and (9)–(11).

derived. No experimental data for similar systems are available for comparison.

A more limited set of experiments was conducted at 383 K. As shown in Fig. 8, the detected profiles are totally different from those recorded at room temperature. Signals identical to those depicted in Figs. 2 and 4 were obtained by reducing the temperature of the mixture to 295 K. The decay observed in the absorption signals clearly demonstrates that $FS(O_2)OOO$ is not formed at 383 K. These experiments can be satisfactorily explained by the proposed mechanism. The simulated absorbances illustrated in Fig. 8 have been evaluated with the rate coefficients given in Table 1. The calculations indicate that the absence of $FS(O_2)OOO$ is almost exclusively due to the marked decrease in the FO_2 concentration as a consequence of thermal dissociation. Indeed, the k_9 value at 383 K is 77 times greater than that at 295 K [48]. Therefore the low FO_2 concentration precludes $FS(O_2)OOOF$ formation through reaction (4). Curves (b) and (c) indicate that the decrease in the absorbance with time can be ascribed to the consumption of FSO_3 radicals in the recombination reactions (1) and (3). Unfortunately, the above-mentioned facts preclude an investigation of the thermal stability of $FS(O_2)OOOF$.

4. Conclusions

The 193 nm photodissociation of FSO_2OF in mixtures with O_2 and the bath gases N_2 and CF_4 was investigated employing the laser flash photolysis technique. A reaction mechanism which explains all the experiments is described. The central species in this scheme is the $FS(O_2)OOO$ radical for which rate coefficients of formation and unimolecular decomposition have been determined at room temperature. A direct characterization of this radical by kinetic and spectroscopic techniques and a more detailed temperature dependence study of the system are planned. In addition, ab initio quantum chemical calculations of the trioxides proposed are desirable.

Acknowledgements

References

[1] J. Czarnowski, E. Castellano and H.J. Schumacher, Z. Phys. Chem. N.F., 57 (1968) 249.

[2] W.H. Basualdo and H.J. Schumacher, Z. Phys. Chem. N.F., 47 (1965) 57.

[3] A.E. Croce de Cobos, C.J. Cobos and E. Castellano, J. Phys. Chem., 93 (1989) 274.

[4] C.J. Cobos, A.E. Croce and E. Castellano, J. Photochem. Photobiol. A: Chem., 59 (1991) 143.

[5] E.H. Staricco, J.E. Sicre and H.J. Schumacher, Z. Phys. Chem. N.F., 35 (1962) 122.

[6] E. Castellano and H.J. Schumacher, Z. Phys. Chem. N.F., 43 (1964) 66.

[7] E. Castellano, R. Gatti, J.E. Sicre and H.J. Schumacher, Z. Phys. Chem. N.F., 42 (1964) 174.

[8] E. Castellano and H.J. Schumacher, Z. Phys. Chem. N.F., 44 (1965) 57.

[9] J.E. Bolzán, J.E. Sicre and H.J. Schumacher, Z. Phys. Chem. N.F., 46 (1965) 78.

[10] R. Gatti and H.J. Schumacher, Z. Phys. Chem. N.F., 62 (1968) 159.

[11] J. Sehested, K. Sehested, O.J. Nielsen and T.J. Wallington, J. Phys. Chem., 98 (1994) 6731.

[12] Z. Li, R.R. Friedl and S.P. Sander, J. Phys. Chem., 99 (1995) 13 445.

[13] C.J. Cobos, A.E. Croce de Cobos, H. Hippler and E. Castellano, J. Phys. Chem., 93 (1989) 3089.

[14] A.E. Croce, C.J. Cobos and E. Castellano, Chem. Phys. Lett., 158 (1989) 157.

[15] C.J. Cobos, A.E. Croce and E. Castellano, Int. J. Chem. Kinet., 22 (1990) 289.

[16] A.E. Croce, J. Photochem. Photobiol. A: Chem., 51 (1990) 293.

[17] C.J. Cobos, A.E. Croce and E. Castellano, in L.M. Narducci, E.J. Quel and J.R. Tredicce (eds.), Lasers and Quantum Optics, CIF Series, Vol. 13, World Scientific, Singapore, 1990, p. 379.

[18] A.E. Croce, C.J. Cobos and E. Castellano, J. Photochem. Photobiol. A: Chem., 55 (1990) 135.

[19] A.E. Croce, C.J. Cobos and E. Castellano, J. Photochem. Photobiol. A: Chem., 64 (1992) 15.

[20] C.J. Cobos, A.E. Croce and E. Castellano, J. Photochem. Photobiol. A: Chem., 84 (1994) 101.

[21] C.J. Cobos, A.E. Croce and E. Castellano, Chem. Phys. Lett., 239 (1995) 320.

[22] C.J. Cobos, A.E. Croce and E. Castellano, J. Fluor. Chem., 79 (1996) 157.

[23] M. Gambaruto, J.E. Sicre and H.J. Schumacher, J. Fluor. Chem., 5 (1975) 175.

[24] G.W. King, D.P. Santry and C.H. Warren, J. Mol. Spectrosc., 32 (1969) 108.

[25] N.M. Matchuk, V.I. Tupikov, A.I. Malkova and S.Ya. Pshezhetskii, Opt. Spectrosc., 40 (1976) 7.

[26] W.B. DeMore, S.P. Sander, D.M. Golden, R.F. Hampson, M.J. Kurylo, C.J. Howard, A.R. Ravishankara, C.E. Kolb and M.J. Molina, Chemical kinetics and photochemical data for use in stratospheric modeling, JPL Publication 94-26, 1994.

[27] S.W. Benson, Thermochemical Kinetics, Wiley, New York, 2nd edn., 1976.

[28] N. Cohen and S.W. Benson, Chem. Rev., 93 (1993) 2419.

[29] S.W. Benson, Chem. Rev., 78 (1978) 23.

[30] J.S. Francisco and I.H. Williams, Int. J. Chem. Kinet., 20 (1988) 455.

[31] T. Rathmann and R.N. Schindler, Chem. Phys. Lett., 190 (1992) 539.

[32] L.R. Anderson and W.P. Fox, J. Am. Chem. Soc., 89 (1967) 4313.

[33] P.G. Thompson, J. Am. Chem. Soc., 89 (1967) 4316.

[34] J. Czarnowski, E. Castellano and H.J. Schumacher, Rev. Latinoam. Quím., 8 (1977) 143.

[35] D.D. DesMarteau and R.M. Hammaker, Isr. J. Chem., 17 (1978) 103.

[36] J. Czarnowski and H.J. Schumacher, J. Fluor. Chem., 12 (1978) 497.

[37] S.W. Benson, J. Am. Chem. Soc., 86 (1964) 3922.

[38] C.M. Rohlfing, Chem. Phys. Lett., 245 (1995) 665.

[39] J.S. Francisco and S.P. Sander, J. Phys. Chem., 100 (1996) 573.

[40] J.S. Francisco, J. Phys. Chem., 99 (1995) 13 422.

[41] K. Sudlow and A.A. Woolf, J. Fluor. Chem., 64 (1993) 269.

[42] R. Gatti, E.H. Staricco, J.E. Sicre and H.J. Schumacher, Angew. Chem., Int. Ed. Engl., 75 (1963) 137.

[43] R. Gatti, E.H. Staricco, J.E. Sicre and H.J. Schumacher, Z. Phys. Chem. N.F., 36 (1963) 211.

[44] I.J. Solomon, A.J. Kacmarek and J. Raney, Inorg. Chem., 7 (1968) 1221.

[45] G.W. King, D.P. Santry and C.H. Warren, J. Chem. Phys., 50 (1969) 4565.

[46] R.W. Fessenden, J. Chem. Phys., 48 (1968) 3725.

[47] J.L. Lyman and R. Holland, J. Phys. Chem., 92 (1988) 7232.

[48] P. Campuzano-Jost, A.E. Croce, H. Hippler, M. Siefke and J. Troe, J. Chem. Phys., 102 (1995) 5317.

[49] K.D. Abney, P.G. Eller, M.P. Eastman, C.F. Pace, S.A. Kinkead, R.J. Kissane and W.H. Woodruff, J. Fluor. Chem., 73 (1995) 137.

[50] A.A. Timakov and V.N. Prusakov, Kinet. Katal., 30 (1989) 472.

[51] G.M. Campbell, J. Fluor. Chem., 46 (1990) 357.

[52] M.M. Maricq, J.J. Szente, T.S. Dibble and J.S. Francisco, J. Phys. Chem., 98 (1994) 12 294.

[53] J. Troe, J. Chem. Phys., 75 (1981) 226.

[54] C.J. Cobos and J. Troe, J. Chem. Phys., 83 (1985) 1010.

[55] C.J. Cobos, unpublished results, 1995.

[56] W. Forst, Theory of Unimolecular Reactions, Academic, New York, 1973.